

Manuscript Number: EJRD-15-01284R1

Title: Dynamic contrast-enhanced and dynamic susceptibility contrast perfusion MR imaging for glioma grading: preliminary comparison of vessel compartment and permeability parameters using hotspot and histogram analysis

Article Type: Research Paper

Keywords: Dynamic contrast-enhanced MRI; Dynamic susceptibility contrast MRI; Perfusion MRI; Glioma; Histogram analysis

Corresponding Author: Dr. Nicoletta Anzalone,

Corresponding Author's Institution: Neuroradiology Unit and CERMAC, San Raffaele Scientific Institute and Vita-Salute San Raffaele University, Milan, Italy

First Author: Corrado Santarosa, MD

Order of Authors: Corrado Santarosa, MD; Antonella Castellano, MD, PhD; Gian Marco Conte, MD; Marcello Cadioli, MSc; Antonella Iadanza, MSc; Maria Rosa Terreni, MD; Alberto Franzin, MD; Lorenzo Bello, MD; Massimo Caulo, MD, PhD; Andrea Falini, MD, PhD; Nicoletta Anzalone

Abstract: Introduction: Dynamic susceptibility contrast (DSC)-MRI is a perfusion technique with high diagnostic accuracy for glioma grading, despite limitations due to inherent susceptibility effects. Dynamic contrast-enhanced (DCE)-MRI has been proposed as an alternative technique able to overcome the DSC-MRI shortcomings.

This pilot study aimed at comparing the diagnostic accuracy of DSC and DCE-MRI for glioma grading by evaluating two estimates of blood volume, the DCE-derived plasma volume (V_p) and the DSC-derived relative cerebral blood volume (rCBV), and a measure of vessel permeability, the DCE-derived volume transfer constant K_{trans} .

Methods: Twenty-six newly diagnosed glioma patients underwent 3T-MR DCE and DSC imaging. Parametric maps of CBV, V_p and K_{trans} were calculated and the region of highest value (hotspot) was measured on each map. Histograms of rCBV, V_p and K_{trans} values were calculated for the tumor volume. Statistical differences according to WHO grade were assessed. The diagnostic accuracy for tumor grading of the two techniques was determined by ROC analysis.

Results: rCBV, V_p and K_{trans} measures differed significantly between high and low-grade gliomas. Hotspot analysis showed the highest correlation with grading. K_{trans} hotspots co-localized with V_p hotspots only in 56% of enhancing gliomas. For differentiating high from low-grade gliomas the AUC was 0.987 for rCBVmax, and 1.000 for V_{pmax} and $K_{transmax}$. Combination of DCE-derived V_p and K_{trans} parameters improved the diagnostic performance of the histogram method.

Conclusion: this initial experience of DCE-derived V_p evaluation shows that this parameter is as accurate as the well-established DSC-derived rCBV for glioma grading. DCE-derived K_{trans} is equally useful for grading, providing different informations with respect to V_p .



OSPEDALE SAN RAFFAELE
ISTITUTO DI RICOVERO E CURA A CARATTERE SCIENTIFICO

Ms. Ref. No.: EJR-D-15-01284R1

Title: DYNAMIC CONTRAST-ENHANCED AND DYNAMIC SUSCEPTIBILITY CONTRAST PERFUSION MR IMAGING FOR GLIOMA GRADING: PRELIMINARY COMPARISON OF VESSEL COMPARTMENT AND PERMEABILITY PARAMETERS USING HOTSPOT AND HISTOGRAM ANALYSIS

Corresponding Author: Dr. Nicoletta Anzalone

Authors: Corrado Santarosa*, MD, Antonella Castellano*, MD, PhD, Gian Marco Conte, MD, Marcello Cadioli, MSc, Antonella Iadanza, MSc, Maria Rosa Terreni, MD, Alberto Franzin, MD, Lorenzo Bello, MD, Massimo Caulo, MD, PhD, Andrea Falini, MD, PhD, Nicoletta Anzalone, MD

Milano, March 8th, 2016

Dear Prof. Blickman,

Please find herewith uploaded the revised version of the manuscript EJR-D-15-01284R1: "DYNAMIC CONTRAST-ENHANCED AND DYNAMIC SUSCEPTIBILITY CONTRAST PERFUSION MR IMAGING FOR GLIOMA GRADING: PRELIMINARY COMPARISON OF VESSEL COMPARTMENT AND PERMEABILITY PARAMETERS USING HOTSPOT AND HISTOGRAM ANALYSIS" by Corrado Santarosa, Antonella Castellano et al.

We are grateful to you and to the two reviewers for all your comments. Our detailed responses to each of the comments are listed below. In the manuscript, changes are marked yellow.

We hope that with these revisions the manuscript will be finally considered suitable for publication in European Journal of Radiology.

Please note that, as previously stated in the title page, Corrado Santarosa and Antonella Castellano contributed equally to this study and share the first authorship.

We thank you for your time and consideration.

Best regards,

Dr. Nicoletta Anzalone, MD

Comments from the Editors and Reviewers:

Reviewer #1

We are grateful to the Referee for his/her comments.

The presented study compares the accuracy of DCE and DSC MR perfusion in glioma grading, by analysing rCBV, Vp and Ktrans, using both hotspot and histogram analysis.

In the studied population DCE derived Vp proved accurate in glioma grading and the results corroborated previous studies suggesting that estimates of blood volume and Ktrans provide different pathophysiologic information and may thus play complimentary roles in the imaging characterization of gliomas.

The subject is important. The study was methodologically well conducted. The article is clearly written.

Response: Thank you.

However, highlights of the article should be provided.

Response: Fixed, thank you. We previously uploaded the highlights as a separate file; we have now embedded them in the manuscript file after the abstract.

The introduction could be more concise (For instance the paragraph on the limitations of the DSC-MRI is too detailed).

Response: Thank you for your suggestion. We have modified and shortened this section accordingly.

Although most of the tables and figures are clear, on Fig 5 b) the ROC curve of maximal Ktrans is difficult to depict.

Response: Fixed, thank you. We have added a third part of the figure (Fig 5c) with the ROC curve of maximal K^{trans} .

Reviewer #3

We are grateful to the Referee for his/her comments.

The authors present their initial experience comparing the diagnostic accuracy of DSC and DCE perfusion evaluation for glioma grading, in a small group of 26 patients (9 low-grade gliomas and 17 high-grade gliomas: 4 AA and 13 GBM).

They have evaluated the DCE-derived plasma volume (Vp), DSC-derived relative cerebral blood volume (rCBV), and a measure of vessel permeability, the DCE derived volume transfer constant. The authors used commercial software (nordicICE - NordicNeuroLab, Bergen, Norway) to generate the parametric maps from which they have calculated the relative and absolute values of the variables abovementioned.

This paper shows some of the advantages of dynamic contrast-enhanced (DCE) MR imaging specially in tumors located in areas prone to susceptibility artefacts and possible for cortical tumors. The statistical analysis is well conducted. The results of the study add further evidence of the added valuable information given by DCE.

The major flaw of this paper is the limited number of patients included precluding it to obtain some meaningful conclusions regarding the differentiation between grades III and IV and between different. Additionally, with the exception of the data on Vp, the other results are well known and the paper adds no relevant new information.

I would consider this paper as a pilot study evaluating the usefulness of Vp and suggest the authors to include this concept (pilot / initial experience of Vp evaluation) on the title / abstract.

Response: Thank you for your suggestion. We have modified the title, the abstract and the

Conclusion paragraph accordingly.

Finally, the quality of figures 2 and 4 is not optimized and is very difficult to evaluate the images "b" on both figures.

Response: Fixed. Thank you.

Potential conflict of interest

Nicoletta Anzalone served as a consultant for Bayer HealthCare and received honorarium and travel reimbursement for meeting related to the study. Marcello Cadioli reports personal fees from Philips Spa and from San Raffaele Scientific Institute, outside the study. All the other authors declare that they have no potential conflict of interest.

European Journal of Radiology Author Form

All manuscripts submitted to the *European Journal of Radiology* must be accompanied by this form. Please scan the form and transmit it to the Editorial Office via EES with the manuscript. If you are unable to do this, please contact the Editorial Office at ejr@elsevier.com to organise an alternative way of sending the form to the Journal.

Title of Manuscript:

Dynamic contrast-enhanced and dynamic susceptibility contrast perfusion MR imaging for glioma grading: comparison of vessel compartment and permeability parameters using hotspot and histogram analysis

Contribution

Author(s)

Study concepts:

Nicoletta Anzalone, Massimo Caulo

Study design:

Nicoletta Anzalone, Massimo Caulo, Antonella Castellano, Corrado Santarosa

Data acquisition:

Nicoletta Anzalone, Massimo Caulo, Antonella Castellano, Corrado Santarosa, Marcello Cadioli, Gian Marco Conte, Antonella Iadanza, Alberto Franzin, Maria Rosa Terreni, Lorenzo Bello

Quality control of data and algorithms:

Nicoletta Anzalone, Massimo Caulo, Antonella Castellano, Corrado Santarosa, Marcello Cadioli, Antonella Iadanza

Data analysis and interpretation:

Nicoletta Anzalone, Massimo Caulo, Antonella Castellano, Corrado Santarosa, Marcello Cadioli, Gian Marco Conte

Statistical analysis:

Antonella Castellano, Gian Marco Conte

Manuscript preparation:

Antonella Castellano, Corrado Santarosa

Manuscript editing:

Nicoletta Anzalone, Massimo Caulo, Andrea Falini

Manuscript review:

Nicoletta Anzalone, Massimo Caulo, Antonella Castellano, Corrado Santarosa, Marcello Cadioli, Gian Marco Conte, Antonella Iadanza, Alberto Franzin, Maria Rosa Terreni, Lorenzo Bello, Andrea Falini

Ethical Approval for Research: Yes

External Funding: No

Possible Conflict of Interest: Yes

(Please ensure that a 'Conflict of Interest' statement is included in your manuscript)

Number of Tables: 8 (incl. 1 supplementary table)

Number of Figures: 5

Name and Title of Corresponding Author: Nicoletta Anzalone, MD

Address: Neuroradiology Unit and CERMAC

San Raffaele Scientific Institute and Vita-Salute San Raffaele University

Via Olgettina 60

Postcode and country: 20132 Milano, Italy

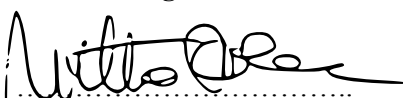
Tel No: +39.02.2643.2236 - 3011

Fax No: +39.02.2643.3447

Email: anzalone.nicoletta@hsr.it

"I confirm that all the authors have made a significant contribution to this manuscript, have seen and approved the final manuscript, and have agreed to its submission to the *European Journal of Radiology*".

Signed (corresponding author):



Date: Milano, October 5th, 2015

Dynamic contrast-enhanced and dynamic susceptibility contrast perfusion MR imaging for glioma grading: preliminary comparison of vessel compartment and permeability parameters using hotspot and histogram analysis

Corrado Santarosa^{1,*}, MD, Antonella Castellano^{1,*}, MD, PhD, Gian Marco Conte¹, MD,
Marcello Cadioli^{1,2}, MSc, Antonella Iadanza¹, MSc,
Maria Rosa Terreni³, MD, Alberto Franzin⁴, MD, Lorenzo Bello⁵, MD,
Massimo Caulo⁶, MD, PhD, Andrea Falini¹, MD, PhD, Nicoletta Anzalone¹, MD

1. Neuroradiology Unit and CERMAC, San Raffaele Scientific Institute and Vita-Salute San Raffaele University, Milan, Italy
2. Philips Healthcare, Monza, Italy
3. Pathology Department, San Raffaele Scientific Institute, Milan, Italy
4. Department of Neurosurgery, San Raffaele Scientific Institute and Vita-Salute San Raffaele University, Milan, Italy
5. Department of Medical Biotechnology and Translational Medicine, Università degli Studi di Milano, Milan, and Humanitas Research Hospital, Rozzano (MI), Italy
6. Department of Neuroscience and Imaging and ITAB-Institute of Advanced Biomedical Technologies, University "G. d'Annunzio", Chieti, Italy

* Corrado Santarosa and Antonella Castellano contributed equally to this study.

Corresponding Author:

Nicoletta Anzalone, MD

Neuroradiology Unit and CERMAC

San Raffaele Scientific Institute and Vita-Salute San Raffaele University

Via Olgettina 60

20132 Milano, Italy

Phone: +39.02.2643.2236 - 3011

Fax: +39.02.2643.3447

Mail: anzalone.nicoletta@hsr.it

Total word count: 3572 words

1
2
3
4 **Dynamic contrast-enhanced and dynamic susceptibility contrast perfusion MR imaging for**
5
6 **glioma grading: **preliminary** comparison of vessel compartment and permeability parameters**
7
8
9 **using hotspot and histogram analysis**
10

11
12
13
14 Manuscript type: Research Paper
15
16
17

18 **Abstract**
19

20
21 **Introduction:** Dynamic susceptibility contrast (DSC)-MRI is a perfusion technique with high
22
23 diagnostic accuracy for glioma grading, despite limitations due to inherent susceptibility effects.
24
25 Dynamic contrast-enhanced (DCE)-MRI has been proposed as an alternative technique able to
26
27 overcome the DSC-MRI shortcomings.
28
29

30
31 This **pilot** study aimed at comparing the diagnostic accuracy of DSC and DCE-MRI for glioma
32
33 grading by evaluating two estimates of blood volume, the DCE-derived plasma volume (Vp) and the
34
35 DSC-derived relative cerebral blood volume (rCBV), and a measure of vessel permeability, the DCE-
36
37 derived volume transfer constant K^{trans} .
38
39

40
41 **Methods:** Twenty-six newly diagnosed glioma patients underwent 3T-MR DCE and DSC
42
43 imaging. Parametric maps of CBV, Vp and K^{trans} were calculated and the region of highest value
44
45 (*hotspot*) was measured on each map. Histograms of rCBV, Vp and K^{trans} values were calculated for the
46
47 tumor volume. Statistical differences according to WHO grade were assessed. The diagnostic accuracy
48
49 for tumor grading of the two techniques was determined by ROC analysis.
50
51

52
53 **Results:** rCBV, Vp and K^{trans} measures differed significantly between high and low-grade
54
55 gliomas. Hotspot analysis showed the highest correlation with grading. K^{trans} hotspots co-localized with
56
57 Vp hotspots only in 56% of enhancing gliomas. For differentiating high from low-grade gliomas the
58
59 AUC was 0.987 for rCBV_{max}, and 1.000 for Vp_{max} and K^{trans}_{max} . Combination of DCE-derived Vp and
60
61
62
63
64
65

1
2
3
4 K^{trans} parameters improved the diagnostic performance of the histogram method.
5
6

7 **Conclusion:** this initial experience of DCE-derived Vp evaluation shows that this parameter is as
8
9 accurate as the well-established DSC-derived rCBV for glioma grading. DCE-derived K^{trans} is equally
10
11 useful for grading, providing different informations with respect to Vp.
12
13
14

15 16 **Keywords**

17
18
19 Dynamic contrast-enhanced MRI - Dynamic susceptibility contrast MRI - Perfusion MRI -
20
21 Glioma - Histogram analysis
22
23
24

25 26 **Highlights**

- 27
28 1. In cerebral gliomas, DCE-MRI is able to overcome DSC-MRI shortcomings.
- 29
30 2. DCE-MRI is as accurate as DSC-MRI for glioma grading.
- 31
32 3. Hotspot and histogram analyses performed equally for glioma grading.
- 33
34 4. The combination of DCE-derived Vp and K^{trans} improves the diagnostic performance.
35
36
37
38
39
40

41 42 **Abbreviations**

43 DCE dynamic contrast-enhanced
44
45 DSC dynamic susceptibility contrast
46
47 MRI magnetic resonance imaging
48
49 LGG low-grade glioma
50
51 HGG high-grade glioma
52
53 rCBV relative cerebral blood volume
54
55 Vp plasma volume
56
57 K^{trans} volume transfer constant
58
59
60
61
62
63
64
65

VIF	vascular input function
ROI	region of interest
ρ	Spearman Rank correlation coefficient
SD	standard deviation
ROC	receiver operating characteristic
AUC	area under the curve

Introduction

Perfusion MR imaging has been the focus of several investigations in neuro-oncology, due to the association between tumor malignancy and neoangiogenesis^{1,2}. In particular, perfusion MR imaging has been used for grading of gliomas which is still based on histopathologic assessment. Nonetheless, histopathologic diagnosis is an invasive procedure and is prone to inherent sampling errors, especially with stereotactic biopsy.

Currently, the most used MR perfusion technique is the dynamic susceptibility contrast (DSC) MR imaging which is based on susceptibility variations during the first pass of a contrast agent bolus through the capillary bed. DSC-MRI allows to estimate the relative cerebral blood volume (rCBV), a parameter that showed a reliable correlation with histopathologic findings of neoangiogenesis³.

Notably, rCBV has been shown to accurately predict WHO histopathologic grading and outcome of patients with brain gliomas^{4,5}. Nevertheless, DSC-MRI is affected by several limitations, such as its sensitivity to magnetic field inhomogeneities⁶ as well as the difficulty to evaluate neoangiogenic hotspots in cortical tumors growing in proximity to large vessels⁷. Moreover, the contrast leakage through a disrupted blood-brain barrier (BBB) may cause an underestimation of the rCBV which should be corrected by using a pre-loading dose of contrast agent, multi-echo sequences or post-processing algorithms^{8,9}. Finally, DSC-MRI does not allow an absolute quantification of tissue

1
2
3
4 perfusion as CBV values must be normalized with respect to contralateral normal brain tissue ¹⁰.
5

6
7 **On the opposite**, dynamic contrast-enhanced (DCE) MR imaging is a perfusion technique based
8
9 on relaxivity variations, as the passage of the contrast agent causes a shortening of T1 relaxation time
10
11 and thus an increase of the T1 signal ¹¹; thus, DCE-MRI is not affected by susceptibility artifacts.
12
13 Moreover, this technique yields an absolute quantification of perfusion parameters and potentially
14
15 allows for a multi-parametric characterization of tumor vasculature ¹¹. The most known DCE-derived
16
17 parameter is the volume transfer constant (K^{trans}) between the intra- and the extra-vascular
18
19 compartments ¹²⁻¹⁵. More recently, pharmacokinetic models allowed to obtain estimates of intra-
20
21 vascular compartment volume such as plasma volume (Vp), derived by the DCE acquisition through
22
23 the extended Tofts and Kermode's model ¹⁶⁻²². Vp is supposed to be a biomarker of tumor
24
25 neoangiogenesis ²⁰.
26
27
28
29
30

31 A few data have been recently available on the comparison of blood volume estimates between
32
33 DCE-derived Vp and DSC-derived rCBV in normal brain and in high-grade tumors ^{20, 21, 23}. Moreover,
34
35 comparison of DCE and DSC parameters on a pixel-by-pixel basis showed only a weak correlation
36
37 between estimates of blood volume (Vp and rCBV) and K^{trans} , thus suggesting that they provide
38
39 different pathological informations ²⁰. Recent reports highlighted the usefulness of DCE perfusion
40
41 imaging in differentiating grade II from grade III gliomas ²⁴, but few data are still available on the role
42
43 of DCE in glioma grading, especially using a pharmacokinetic model to estimate the intra-vascular
44
45 compartment volume.
46
47
48
49

50 The primary aim of this study was to compare the diagnostic accuracy of two estimates of blood
51
52 volume, the DCE-derived Vp and DSC-derived rCBV in pre-treatment glioma grading, using both a
53
54 region-of-interest (ROI) and an histogram analysis. Additionally, a comparison of the DCE-derived
55
56 volume transfer constant K^{trans} and the two estimates of blood volume Vp and rCBV was also
57
58 performed with respect to glioma grading.
59
60
61
62
63
64
65

1
2
3
4
5 **Methods**
6

7 *Patient population*
8
9

10 This prospective study was approved by the ethical committees of our Institutions and prior
11 written informed consent was obtained from all patients.
12
13

14
15 A total of 26 adult patients (mean age, 55.4 years; range, 22-79 years; 15M/11F) presenting at our
16 Institutions with a newly detected brain lesion suggestive of glioma were prospectively enrolled in this
17 study. Demographic data of all the patients are summarized in Table 1. Exclusion criteria were the
18 presence of a severe renal failure and a known allergy to gadolinium-based contrast agent. Patients
19 underwent a single pre-operative MR session including conventional sequences and perfusion DSC and
20 DCE imaging.
21
22
23
24
25
26
27
28

29 An experienced neuropathologist provided histopathologic diagnosis according to the World
30 Health Organization (WHO) 2007 classification.
31
32

33
34 *MR Imaging*
35

36
37 MR imaging was performed on a 3T scanner (Achieva, Philips Healthcare, Best, the Netherlands)
38 equipped with 80 mT/m gradients using a phased-array head 8 channel-coil. Table 2 summarizes the
39 imaging parameters of the MRI sequence protocol.
40
41
42
43

44 DCE-MR imaging was performed with a dynamic gradient-echo T1-weighted sequence using the
45 following parameters: TR/TE, 3.9/1.8 ms; flip angle, 15°; matrix, 96×84; field of view (FOV),
46 230×201 mm; section thickness, 2.5 mm; in-plane acquisition voxel size, 2.4×2.4 mm. A total of 70
47 dynamic scans were performed with a temporal resolution of 5.1 seconds. The total acquisition time for
48 DCE-MRI was 6 minutes and 10 seconds. DCE-MRI was preceded by a Variable Flip Angle axial
49 sequence for T1 mapping.
50
51
52
53
54
55
56
57

58
59 DSC-MR imaging was performed with an axial gradient-echo T2*-weighted echo-planar (EPI)
60 sequence by using the following parameters: TR/TE, 1500/40 ms; flip angle, 75°; matrix, 96×77 mm;
61
62
63
64
65

1
2
3
4 FOV, 230×230 mm; section thickness, 5 mm; in-plane acquisition voxel size, 2.4×2.9. A total of 80
5
6 dynamic scans were performed with a temporal resolution of 1.5 seconds. The total acquisition time for
7
8 DSC-MRI was 2 minutes and 4 seconds.
9

10
11 A cumulative fixed dose of 10 mL of gadobutrol (Gadovist, 1 mmol/mL; Bayer Schering Pharma,
12
13 Berlin, Germany) was administered, splitted in two bolus of 5 mL. The first bolus of 5 mL was injected
14
15 50 seconds after the start of the DCE sequence by using a power injector (Spectris Solaris MR injector;
16
17 MedRad, Indianola, Pennsylvania) at a rate of 2 mL/s, immediately followed by a 20 ml continuous
18
19 saline flush at the same injection rate. The second bolus of 5 ml was injected 16 seconds after the start
20
21 of the DSC sequence by using the same power injector at a rate of 5 mL/s, followed by a 20 ml saline
22
23 flush at the same injection rate. Thus, the contrast administration during DCE sequence pre-saturated
24
25 the tissue for the following DSC-MR imaging.
26
27
28
29

30 31 *Image analysis*

32
33 DCE and DSC perfusion MRI data were processed on an independent workstation by using the
34
35 software nordicICE (NordicNeuroLab, Bergen, Norway).
36
37

38 DCE. The maps of pharmacokinetic parameters V_p and K^{trans} were calculated from DCE
39
40 sequence using the extended two-compartment pharmacokinetic Tofts and Kermode's model, which
41
42 yields estimates of plasma volume (V_p) and K^{trans} ²². Deconvolution with a vascular input function
43
44 (VIF) was performed. The VIF was measured from a region of interest (ROI) positioned in the superior
45
46 sagittal sinus of each patient. The ROI was drawn *in consensus* by a resident radiologist (with two
47
48 years of experience in neuroradiology) and a board-certified neuroradiologist (with more than 20 years
49
50 of experience). Patient-specific baseline T1 maps were derived from VFA sequences using a dedicated
51
52 nordicICE software processing module.
53
54
55
56

57 DSC. The CBV maps were calculated using an established tracer kinetic model applied to the
58
59 first-pass data, as implemented in nordicICE software. A mathematical correction was applied to the
60
61
62
63
64
65

1
2
3
4 dynamic curves in order to compensate for contrast-agent leakage effects⁹. The contrast bolus
5
6 administered during the DCE acquisition worked as an additional stratagem to compensate for the T1
7
8 contamination of the DSC sequences.
9

10
11 Conventional MR images and perfusion parametric maps were revised by a resident radiologist
12
13 and a board-certified neuroradiologist *in consensus*, both blinded to histopathologic diagnosis. DCE
14
15 and DSC-derived parametric perfusion maps were automatically coregistered to the 3D-FLAIR and
16
17 post-contrast 3D-T1 images by performing a rigid transformation of the datasets, in order to accurately
18
19 define the tumor borders.
20
21

22
23 The region of maximal abnormality within the lesion volume (*hotspot*) was determined with a
24
25 visual inspection on each parametric map (CBV, Vp and K^{trans}). Four separate ROIs with an area of 25-
26
27 30 mm² were placed on the hotspot, avoiding intra-tumoral blood vessels, and the maximum value for
28
29 each parameter (CBV_{max}, Vp_{max} and $K^{\text{trans}}_{\text{max}}$) was recorded. The maximum CBV value was divided by
30
31 the CBV value of an ROI positioned in the contralateral normal-appearing white matter to compute
32
33 rCBV_{max}.
34
35

36
37 The co-localization of the tumor hotspots with maximal rCBV and Vp values and maximal Vp
38
39 and K^{trans} values was also investigated. The observation of a spatial overlap between two hotspots after
40
41 rigid coregistration of perfusion maps defined the co-localization of the hotspots.
42
43
44

45
46 In patients with contrast enhancing tumors the segmentation of the tumor volume was performed
47
48 using the perfusion-coregistered post-contrast 3D-T1 FFE images, whereas in patients with non-
49
50 enhancing tumor the 3D-FLAIR images were used. Cystic or necrotic regions, intra-tumoral vessels
51
52 and definite perilesional edema were excluded from the segmentation. Tumor segmentations were
53
54 merged to the corresponding coregistered perfusion maps. rCBV, Vp and K^{trans} values of the segmented
55
56 volumes were extracted and plotted as histograms, whose main parameters were obtained: mean,
57
58 median, standard deviation, skewness, kurtosis, 90th and 95th percentiles.
59
60
61
62
63
64
65

1
2
3
4 *Statistical analysis*
5

6
7 The Shapiro-Wilk's test was used to test normality of the data. Group differences of both
8
9 hotspots and histogram perfusion parameters according to histopathologic WHO grade were assessed
10
11 using the Mann-Whitney U test and Bonferroni correction for multiple comparisons. The Spearman's
12
13 rank correlation coefficients (ρ) were used to assess the relationships between intra-patient $rCBV_{max}$
14
15 and K^{trans}_{max} values, Vp_{max} and K^{trans}_{max} values, and $rCBV_{max}$ and Vp_{max} values. Spearman's ρ test was
16
17 also used to assess the association between both hotspot and histogram perfusion parameters and WHO
18
19 grade.
20
21
22

23
24 Receiver operating characteristic (ROC) curve analysis was used to evaluate the performance of
25
26 each parameter in discriminating high-grade from low-grade gliomas, by comparing the area under the
27
28 curve (AUC). A logistic regression analysis and receiver-operating characteristic (ROC) curves were
29
30 calculated by combining different histogram parameters, to determine their added value for predicting
31
32 glioma grading.
33
34

35
36 Analysis and statistical figures were calculated using SPSS 20.0 for MacOSX (SPSS Inc., IBM,
37
38 Chicago, IL) and MedCalc software, version 15 (MedCalc Software, Ostend, Belgium).
39
40
41

42
43 **Results**
44

45 *Patient population*
46

47
48 Of the 26 patients enrolled in this study 9 presented with a low-grade WHO II glioma (LGGs)
49
50 and 17 with a high-grade gliomas (HGGs: WHO III gliomas, $n = 4$; WHO IV glioblastoma, $n = 13$).
51

52
53 Detailed histopathological data of all the patients are reported in Table 1.
54

55 *Hotspot analysis*
56

57
58 The median $rCBV_{max}$, Vp_{max} and K^{trans}_{max} values and ranges for WHO grade II, III and IV tumors
59
60 are shown in Table 3 and Figure 1. The difference between the median values of grade II and grade III
61
62
63
64
65

1
2
3
4 glioma hotspot values were statistically significant both for DSC-derived $rCBV_{max}$ ($P=0.017$) and
5
6 DCE-derived Vp_{max} and K^{trans}_{max} ($P=0.008$). A statistically significant difference between grade III and
7
8 grade IV gliomas was found in median Vp_{max} values ($P=0.018$) whereas median $rCBV_{max}$ and median
9
10 K^{trans}_{max} values did not differ significantly ($P>0.05$). Median values of each hotspot parameter were
11
12 significantly different between LGGs and HGGs ($P<0.0001$). Figure 2 and 3 show an example of a
13
14 LGG and a HGG, respectively.
15
16

17
18 Spearman's rank correlation test revealed statistically significant relationships between intra-
19
20 patient $rCBV_{max}$ and Vp_{max} values ($\rho = 0.727, P<0.0001$), between $rCBV_{max}$ and K^{trans}_{max} values ($\rho =$
21
22 $0.747, P<0.0001$) and between Vp_{max} and K^{trans}_{max} values ($\rho = 0.829, P<0.0001$). With respect to glioma
23
24 grade, each perfusion parameter had a highly significant positive correlation ($P<0.0001$) with
25
26 Spearman's rank correlation coefficients of $\rho = 0.761$ for $rCBV_{max}$, $\rho = 0.893$ for Vp_{max} and $\rho = 0.818$
27
28 for K^{trans}_{max} (Table 4).
29
30
31
32

33
34 In 24 out of 26 gliomas (92%) a spatial correspondence between $rCBV_{max}$ and Vp_{max} hotspots
35
36 was observed. In the 2 cases where $rCBV_{max}$ and Vp_{max} hotspots did not co-localize, susceptibility
37
38 variations on $rCBV$ maps masked the region where the maximal abnormality was found on Vp maps
39
40 (Figure 4).
41

42
43 Tumor K^{trans} values consistently differed from those of normal appearing white matter only in
44
45 enhancing regions. K^{trans} hotspots co-localized with Vp hotspots in 10 out of 18 (56%) enhancing
46
47 gliomas, while they did not co-localize in the remaining 8 enhancing gliomas.
48
49

50 *Histogram analysis*

51
52 Histogram parameters for LGGs and HGGs and for WHO grade II, III and IV tumors are shown
53
54 in Table 5, Figure 1d-f and Supplementary Table 1, respectively.
55
56

57
58 In DSC-derived $rCBV$ histograms, pairwise comparisons demonstrated statistically significant
59
60 differences of mean, median, standard deviation, 90th and 95th percentiles between LGGs and HGGs
61
62
63
64
65

1
2
3
4 (Table 5, $P<0.05$); the lowest p -value was found for mean values ($P=0.001$).
5
6

7 In DCE-derived maps, LGGs and HGGs showed Bonferroni-corrected highly significant
8
9 statistical differences with respect to the following Vp histogram parameters (Table 5, $P<0.001$): mean,
10
11 median, 90th and 95th percentiles, while differences in skewness and kurtosis were less significant
12
13 ($P<0.05$). Finally, all the K^{trans} histogram parameters were highly significantly different between LGGs
14
15 and HGGs (Table 5, $P<0.005$): the lowest p -value was found for mean and 90th percentile values
16
17 ($P\leq 0.0001$).
18
19
20

21 With respect to glioma grade, each DCE-derived histogram parameter had a highly significant
22
23 Bonferroni-corrected positive correlation (Table 6, $P<0.0001$), with highest Spearman's rank
24
25 correlation coefficients of $\rho = 0.795$ for mean Vp and $\rho = 0.702$ for 90th percentiles K^{trans} . DSC-derived
26
27 rCBV histogram parameter had significant positive correlation ($P<0.0001$) with tumor grade as well,
28
29 with highest Spearman's rank correlation coefficients of $\rho = 0.705$ for mean rCBV.
30
31
32

33 *ROC curve analysis*

34
35 Table 7 and Figure 5 show the area under the ROC curves, proportional to diagnostic accuracy,
36
37 of each DSC- and DCE-derived histogram parameter for differentiating HGGs from LGGs. In DSC, the
38
39 mean and 90th percentiles rCBV values had the highest AUC (0.928 and 0.895, respectively). In DCE-
40
41 derived Vp histograms, the mean and 90th percentiles had the highest AUC (0.954 and 0.948,
42
43 respectively). In K^{trans} histograms, the mean and 90th percentiles had the highest AUC (0.980 and 0.967,
44
45 respectively) for separating LGGs from HGGs. Combination of DCE-derived Vp and K^{trans} and DSC-
46
47 derived rCBV histogram parameters improved the diagnostic performance of the histogram method
48
49 (Table 7 and Figure 5a), approaching an AUC value of 1.
50
51
52
53

54
55 Using the hotspot method for differentiating HGGs from LGGs the area under the ROC curves
56
57 was 0.987 (CI: 0.844-1.000, $P<0.0001$) for rCBV_{max}, 1.000 (CI: 0.868-1.000, $P<0.0001$) for Vp_{max} and
58
59 1.000 (CI: 0.868-1.000, $P<0.0001$) for K^{trans} _{max} (Figure 5b). The differences between the AUCs were
60
61
62
63
64
65

1
2
3
4 not statistically significant ($P=0.54$).
5

6 An $rCBV_{max}$ cut-off value of 1.85, associated to a sensitivity of 100% and a specificity of 90%,
7
8 allowed to correctly identify all the HGGs (17/17) and 9/10 LGGs. The misclassified low grade glioma
9
10 was a left frontal oligoastrocytoma with extensive cortical involvement (Figure 4).
11
12

13 A Vp_{max} cut-off value of 2.25 mL/100 g, associated to a sensitivity and a specificity of 100%,
14
15 allowed for a correct grading of all high grade (17/17) and low grade gliomas (10/10). When compared
16
17 to $rCBV$, the proposed Vp cut-off value increased specificity, allowing to correctly classify the
18
19 aforementioned low-grade oligoastrocytoma. A K_{max}^{trans} cut-off value of 0.019 minutes⁻¹ was also
20
21 associated to a sensitivity and specificity of 100%.
22
23
24
25

26 27 **Discussion**

28
29 This study demonstrates that DCE-derived Vp is an effective and accurate parameter for glioma
30
31 grading in a pre-operative setting, using both the *hotspot* method and histogram analysis. It also
32
33 suggests the utility of DCE-derived volume transfer constant K^{trans} as an additional and complementary
34
35 parameter to further improve grading accuracy.
36
37
38

39 DCE-MRI has recently been suggested for brain tumor grading by using volume transfer constant
40
41 K^{trans} and Vp . A few data have been recently available on the accuracy of these DCE-derived measures
42
43 in determining glioma grading, even if they seem both promising^{20, 21, 24}. Alcaide-Leon et al. recently
44
45 demonstrated a significant correlation between the two estimates of microvascular density $rCBV$ and
46
47 Vp in a small serie of high grade gliomas on a pixel-by-pixel basis²⁰.
48
49
50

51 Our **initial experience** indicates that the maximal abnormality of DCE-derived Vp showed the
52
53 same accuracy of the most commonly used DSC-derived $rCBV$ in predicting glioma grading, by using
54
55 both the hotspot method and histogram analysis. Benefits of DCE Vp consisted in the ability to
56
57 evaluate perfusion in the whole tumor volume, regardless of the tumor location and the presence of
58
59 hemorrhagic foci, and to discriminate more easily surrounding macro-vessel from true intralesional
60
61
62
63
64
65

1
2
3
4 neoangiogenic hotspots. In fact, DCE-derived Vp and DSC-derived rCBV performed equally well in
5
6 grading each lesion of our sample except for a left frontal low-grade oligoastrocytoma (Figure 4) with
7
8 extensive cortical involvement, whose grade was correctly assessed by Vp but not by rCBV. Hotspots
9
10 were located in a parasagittal region of the lesion, showing a high rCBV_{max} of 5 and, in the same ROI,
11
12 a Vp_{max} of 1.9 mL/100 g, which was similar to the median Vp values of LGGs than that of HGGs. It is
13
14 likely that this tumor region had extremely elevated rCBV values because of large susceptibility
15
16 variations in adjacent venous vessel and cortical macro-vessels, overcoming the contribution from the
17
18 lesion vasculature itself. Moreover, it is well known from previous studies that oligodendrogliomas
19
20 may have elevated rCBV values irrespective of glioma grade²⁵. This is supposed to be related to their
21
22 microvessel network pattern, named "chickenwire". However it cannot be excluded that their extremely
23
24 high rCBV values are more related to their cortical location and proximity to cortical vessel than to the
25
26 characteristic tumor neoangiogenesis, at least for low-grade oligodendrogliomas. By overcoming
27
28 macrovessels susceptibility effects, DCE-MRI may reduce the overlap between low-grade and high-
29
30 grade oligodendrogliomas, increasing the accuracy in glioma grade prediction, but this should be
31
32 investigated in larger studies.
33
34
35
36
37
38
39

40
41 Hotspot analysis by experienced operators shows the highest correlation with tumor grade for all
42
43 the explored parameters. This *hotspot* method has been demonstrated to provide the highest inter-
44
45 observer and intra-observer reproducibility in perfusion measurements²⁶. The accuracy of histogram
46
47 metrics approaches that of hotspot analysis (Table 5 and 6) and may be useful for obtaining robust and
48
49 comparable DCE measures also by inexperienced operators, as previously described for rCBV
50
51 histograms by Law et al.²⁷.
52
53
54

55
56 The difference between the median values of grade II and grade III glioma hotspot values were
57
58 statistically significant for DCE-derived Vp_{max} and $K^{\text{trans}}_{\text{max}}$ ($P=0.008$), as well as for DSC-derived
59
60 rCBV_{max} ($P=0.017$). This is in line with recent reports demonstrating the usefulness of DCE perfusion
61
62
63
64
65

1
2
3
4 imaging in differentiating grade II from grade III gliomas²⁴. Moreover, despite the limited number of
5
6 cases with grade III gliomas, a statistically significant difference between grade III and grade IV
7
8 gliomas was found in median $V_{p_{max}}$ values ($P=0.018$), whereas we did not find a statistically
9
10 significant difference between these two groups by using $rCBV_{max}$ or K^{trans}_{max} values ($P>0.05$) (Table 3).
11
12 The small number of WHO III gliomas included in this series prevent us from drawing any definitive
13
14 conclusion, as a larger sample size is needed to confirm an outperformance of DCE-derived V_p over
15
16 DSC-derived $rCBV$ in discriminating grade III from grade IV gliomas. However, some theoretical
17
18 considerations may support the idea that DCE may better detect small variations in tumor perfusion,
19
20 thus reducing the overlap of the two groups. In fact, the T2*-weighted DSC signal variation in a given
21
22 voxel does not rely only on the local contrast distribution volume as the T1-weighted DCE signal
23
24 variation, but it is also affected by the vessel diameter and spacing and by the susceptibility of adjacent
25
26 voxels²⁸.
27
28
29
30
31

32
33 In our study K^{trans} was also measured, as it is the most commonly DCE-derived parameter in
34
35 literature¹²⁻¹⁵. This allows an extensive comparison of our results with previous data, thus validating
36
37 our DCE-MRI protocol and data processing. In our series, K^{trans} was confirmed to be a good predictor
38
39 of glioma grading, even though we found that K^{trans} hotspots co-localized with V_p hotspots only in 56%
40
41 of enhancing gliomas. This result is in line with recent data obtained from a pixel-by-pixel comparison
42
43 of K^{trans} and CBV values in high-grade gliomas, that show a very weak positive correlation between
44
45 these two parameters²⁰. This low correlation suggests that V_p and K^{trans} provide different physiologic
46
47 information, as vessel permeability is a property of tumor vasculature at least in part independent from
48
49 the increasing of tumor vessel volume. Moreover, the combination of DCE-derived V_p and K^{trans}
50
51 histogram parameters improved the diagnostic performance of the histogram method on DCE
52
53 parameters (Table 7), further supporting this hypothesis.
54
55
56
57
58
59

60 This study has some limitations, such as the small number of enrolled patients and the
61
62
63
64
65

1
2
3
4 composition of our sample. Specifically, only four grade III gliomas were included, mainly due to their
5
6 low incidence. In addition only one low-grade oligoastrocitoma with high rCBV values was included in
7
8 our sample, that prevents from any generalization about the supposed advantage of DCE over DSC in
9
10 oligodendroglioma grading: this result must be confirmed in a larger cohort of patients.
11
12

13
14 Regarding the methodology, the vascular input function was selected from superior sagittal sinus
15
16 on magnitude images, thus limiting the quantitative value of DCE parameters: however, a general
17
18 agreement on this issue has not been achieved, still being a matter of debate^{29, 30}. In addition, a formal
19
20 interobserver data analysis should be added to estimate the reliability and reproducibility of DCE-
21
22 derived measures with respect to DSC-derived rCBV.
23
24
25
26
27

28 **Conclusion**

29
30 This **pilot** study demonstrates that DCE-derived Vp, an estimate of tumor neoangiogenesis,
31
32 performs similarly to the DSC-derived rCBV in glioma grading using both region-of-interest (ROI) and
33
34 histogram analysis. Additionally, the role of DCE-derived K^{trans} as a predictor of glioma grading is
35
36 also supported by our data. The combination of DCE-derived Vp and K^{trans} and DSC-derived rCBV
37
38 histogram parameters improves the diagnostic performance of perfusion imaging.
39
40
41
42

43 Though promising, these data need to be confirmed in a larger cohort of patients before
44
45 considering DCE as an alternative or complementary perfusion MRI tool for glioma grading. Moreover,
46
47 further efforts are needed to standardize DCE acquisitions and post-processing in a multi-center
48
49 environment, in order to widely implement this technique in a clinical setting.
50
51
52
53
54

55 **Acknowledgements**

56
57 **The Authors are grateful to Gianluca Brugnara for help in image preparation.**
58
59
60
61
62
63
64
65

1
2
3
4 **References**
5
6

7 [1] Brem S, Cotran R, Folkman J. Tumor angiogenesis: a quantitative method for histologic
8 grading. J Natl Cancer Inst 1972;48(2):347-56.
9

10 [2] Leon SP, Folkerth RD, Black PM. Microvessel density is a prognostic indicator for patients
11 with astroglial brain tumors. Cancer 1996;77(2):362-72.
12
13

14 [3] Sadeghi N, D'Haene N, Decaestecker C, et al. Apparent diffusion coefficient and cerebral
15 blood volume in brain gliomas: relation to tumor cell density and tumor microvessel density based on
16 stereotactic biopsies. AJNR Am J Neuroradiol 2008;29(3):476-82.
17
18
19

20 [4] Law M, Yang S, Wang H, et al. Glioma grading: sensitivity, specificity, and predictive values
21 of perfusion MR imaging and proton MR spectroscopic imaging compared with conventional MR
22 imaging. AJNR Am J Neuroradiol 2003;24(10):1989-98.
23
24
25

26 [5] Law M, Young RJ, Babb JS, et al. Gliomas: predicting time to progression or survival with
27 cerebral blood volume measurements at dynamic susceptibility-weighted contrast-enhanced perfusion
28 MR imaging. Radiology 2008;247(2):490-8.
29
30
31

32 [6] Lacerda S, Law M. Magnetic resonance perfusion and permeability imaging in brain tumors.
33 Neuroimaging Clin N Am 2009;19(4):527-57.
34
35
36

37 [7] Sugahara T, Korogi Y, Kochi M, Ushio Y, Takahashi M. Perfusion-sensitive MR imaging of
38 gliomas: comparison between gradient-echo and spin-echo echo-planar imaging techniques. AJNR Am
39 J Neuroradiol 2001;22(7):1306-15.
40
41
42

43 [8] Hu LS, Baxter LC, Pinnaduwa DS, et al. Optimized preload leakage-correction methods to
44 improve the diagnostic accuracy of dynamic susceptibility-weighted contrast-enhanced perfusion MR
45 imaging in posttreatment gliomas. AJNR Am J Neuroradiol 2010;31(1):40-8.
46
47
48
49
50
51
52
53
54
55
56
57
58
59
60
61
62
63
64
65

1
2
3
4 [9] Boxerman JL, Schmainda KM, Weisskoff RM. Relative cerebral blood volume maps
5
6 corrected for contrast agent extravasation significantly correlate with glioma tumor grade, whereas
7
8 uncorrected maps do not. *AJNR Am J Neuroradiol* 2006;27(4):859-67.
9

10
11 [10] Ostergaard L. Principles of cerebral perfusion imaging by bolus tracking. *J Magn Reson*
12
13 *Imaging* 2005;22(6):710-7.
14

15
16 [11] Larsson HB, Hansen AE, Berg HK, Rostrup E, Haraldseth O. Dynamic contrast-enhanced
17
18 quantitative perfusion measurement of the brain using T1-weighted MRI at 3T. *J Magn Reson Imaging*
19
20 2008;27(4):754-62.
21

22
23 [12] Jia Z, Geng D, Xie T, Zhang J, Liu Y. Quantitative analysis of neovascular permeability in
24
25 glioma by dynamic contrast-enhanced MR imaging. *J Clin Neurosci* 2012;19(6):820-3.
26

27
28 [13] Patankar TF, Haroon HA, Mills SJ, et al. Is volume transfer coefficient ($K(\text{trans})$) related to
29
30 histologic grade in human gliomas? *AJNR Am J Neuroradiol* 2005;26(10):2455-65.
31

32
33 [14] Roberts HC, Roberts TP, Brasch RC, Dillon WP. Quantitative measurement of
34
35 microvascular permeability in human brain tumors achieved using dynamic contrast-enhanced MR
36
37 imaging: correlation with histologic grade. *AJNR Am J Neuroradiol* 2000;21(5):891-9.
38

39
40 [15] Zhang N, Zhang L, Qiu B, Meng L, Wang X, Hou BL. Correlation of volume transfer
41
42 coefficient K_{trans} with histopathologic grades of gliomas. *J Magn Reson Imaging* 2012;36(2):355-63.
43

44
45 [16] Zhang Y, Wang J, Wang X, Zhang J, Fang J, Jiang X. Feasibility study of exploring a T(1)-
46
47 weighted dynamic contrast-enhanced MR approach for brain perfusion imaging. *J Magn Reson*
48
49 *Imaging* 2012;35(6):1322-31.
50

51
52 [17] Harrer JU, Parker GJ, Haroon HA, et al. Comparative study of methods for determining
53
54 vascular permeability and blood volume in human gliomas. *J Magn Reson Imaging* 2004;20(5):748-57.
55
56
57
58
59
60
61
62
63
64
65

1
2
3
4 [18] Awasthi R, Rathore RK, Soni P, et al. Discriminant analysis to classify glioma grading using
5
6 dynamic contrast-enhanced MRI and immunohistochemical markers. *Neuroradiology* 2012;54(3):205-
7
8 13.

9
10
11 [19] Mills SJ, Patankar TA, Haroon HA, Baleriaux D, Swindell R, Jackson A. Do cerebral blood
12
13 volume and contrast transfer coefficient predict prognosis in human glioma? *AJNR Am J Neuroradiol*
14
15 2006;27(4):853-8.

16
17
18 [20] Alcaide-Leon P, Pareto D, Martinez-Saez E, Auger C, Bharatha A, Rovira A. Pixel-by-Pixel
19
20 Comparison of Volume Transfer Constant and Estimates of Cerebral Blood Volume from Dynamic
21
22 Contrast-Enhanced and Dynamic Susceptibility Contrast-Enhanced MR Imaging in High-Grade
23
24 Gliomas. *AJNR Am J Neuroradiol* 2015;36(5):871-6.

25
26
27 [21] Artzi M, Liberman G, Nadav G, et al. Human cerebral blood volume measurements using
28
29 dynamic contrast enhancement in comparison to dynamic susceptibility contrast MRI. *Neuroradiology*
30
31 2015;57(7):671-8.

32
33
34 [22] Tofts PS, Brix G, Buckley DL, et al. Estimating kinetic parameters from dynamic contrast-
35
36 enhanced T(1)-weighted MRI of a diffusable tracer: standardized quantities and symbols. *J Magn*
37
38 *Reson Imaging* 1999;10(3):223-32.

39
40
41 [23] Nguyen TB, Cron GO, Perdrizet K, et al. Comparison of the Diagnostic Accuracy of DSC-
42
43 and Dynamic Contrast-Enhanced MRI in the Preoperative Grading of Astrocytomas. *AJNR Am J*
44
45 *Neuroradiol* 2015.

46
47
48 [24] Falk A, Fahlstrom M, Rostrup E, et al. Discrimination between glioma grades II and III in
49
50 suspected low-grade gliomas using dynamic contrast-enhanced and dynamic susceptibility contrast
51
52 perfusion MR imaging: a histogram analysis approach. *Neuroradiology* 2014;56(12):1031-8.

53
54
55 [25] Lev MH, Ozsunar Y, Henson JW, et al. Glial tumor grading and outcome prediction using
56
57 dynamic spin-echo MR susceptibility mapping compared with conventional contrast-enhanced MR:
58
59

1
2
3
4 confounding effect of elevated rCBV of oligodendrogliomas [corrected. AJNR Am J Neuroradiol
5
6 2004;25(2):214-21.
7

8
9 [26] Wetzel SG, Cha S, Johnson G, et al. Relative cerebral blood volume measurements in
10
11 intracranial mass lesions: interobserver and intraobserver reproducibility study. Radiology
12
13 2002;224(3):797-803.
14

15
16 [27] Law M, Young R, Babb J, Pollack E, Johnson G. Histogram analysis versus region of
17
18 interest analysis of dynamic susceptibility contrast perfusion MR imaging data in the grading of
19
20 cerebral gliomas. AJNR Am J Neuroradiol 2007;28(4):761-6.
21

22
23 [28] Kiselev VG. On the theoretical basis of perfusion measurements by dynamic susceptibility
24
25 contrast MRI. Magn Reson Med 2001;46(6):1113-22.
26

27
28 [29] Ewing JR, Bagher-Ebadian H. Model selection in measures of vascular parameters using
29
30 dynamic contrast-enhanced MRI: experimental and clinical applications. NMR in biomedicine
31
32 2013;26(8):1028-41.
33

34
35 [30] Nguyen TB, Cron GO, Mercier JF, et al. Diagnostic accuracy of dynamic contrast-enhanced
36
37 MR imaging using a phase-derived vascular input function in the preoperative grading of gliomas.
38
39 AJNR Am J Neuroradiol 2012;33(8):1539-45.
40
41

42 43 44 45 **Image captions**

46
47
48 **Fig 1 (a-c)** Region of maximal abnormality (*hotspot*) values of rCBV, Vp and K^{trans} for WHO
49
50 grade II, III and IV tumors. Dot-plots (median and range) showing (a) rCBV_{max} , (b) Vp_{max} , and (c)
51
52 $K^{\text{trans}}_{\text{max}}$ values in different tumor grades. (d-f) Histogram values of the best DSC- and DCE-derived
53
54 histogram parameters for differentiating HGGs from LGGs (see Table 5), compared to hotspot
55
56 maximal values. Dot-plots (median and range) showing (d) mean and 90th percentile of rCBV values
57
58 and corresponding hotspot rCBV measures, (e) mean and 90th percentile of Vp values and
59
60
61
62
63
64
65

1
2
3
4 corresponding hotspot Vp measures, (f) mean and 90th percentile of K^{trans} values and corresponding
5
6 hotspot K^{trans} measures. * $P \leq 0.05$, ** $P \leq 0.01$, *** $P \leq 0.001$, **** $P \leq 0.0001$
7
8
9

10
11 **Fig 2** A case of left frontal astrocytoma WHO grade II. (a) FLAIR image, (b) K^{trans} map (c) CBV
12 map and (d) Vp map. The lesion shows a low $rCBV_{\text{max}}$ of 0.9 (red arrow), a low Vp_{max} of 0.6 mL/100 g
13 (yellow arrow) and a low $K^{\text{trans}}_{\text{max}}$ of 0.005 min^{-1} (blue arrow). Note the presence of a right frontal
14 venous anomaly represented as an area of elevated CBV beside the vessel as it appears on
15 morphological images and on the Vp map.
16
17
18
19
20
21
22
23
24
25

26 **Fig 3** A case of right fronto-insular glioblastoma WHO grade IV. (a) Post-contrast T1-w image,
27 (b) K^{trans} map (c) CBV map and (d) Vp map. The lesion shows a high $rCBV_{\text{max}}$ of 6.5 (red arrow), a
28 high maximal Vp of 6.1 mL/100 g (yellow arrow) and a high $K^{\text{trans}}_{\text{max}}$ of 0.11 min^{-1} (blue arrow). DCE
29 maps allow to identify a focal area of higher Vp and K^{trans} values within the lesion, not clearly
30 distinguishable on CBV map.
31
32
33
34
35
36
37
38
39
40

41 **Fig 4** A case of left frontal parasagittal oligoastrocytoma WHO grade II. (a) Post-contrast T1-w
42 image, (b) K^{trans} map (c) CBV map and (d) Vp map. The lesion shows a high $rCBV_{\text{max}}$ of 5 (red arrow),
43 a low Vp_{max} of 1.9 mL/100 g (yellow arrow) and a low $K^{\text{trans}}_{\text{max}}$ of 0.016 min^{-1} (blue arrow). The
44 presence of a prominent venous vessel and adjacent cortical macro-vessels cause large susceptibility
45 variations hampering a correct identification of the lesion, clearly shown on DCE Vp and Ktrans map.
46
47
48
49
50
51
52
53
54

55 **Fig 5** Comparison of ROC curves of (a) combined DCE and DSC-derived histogram measures
56 and (b) and (c) hotspot values for differentiating HGGs from LGGs (see Table 7).
57
58
59
60
61
62
63
64
65

1
2
3
4
5
6
7
8
9
10
11
12
13
14
15
16
17
18
19
20
21
22
23
24
25
26
27
28
29
30
31
32
33
34
35
36
37
38
39
40
41
42
43
44
45
46
47
48
49
50
51
52
53
54
55
56
57
58
59
60
61
62
63
64
65

Table 1. Clinical and histopathological details of the patients' population.

Patient #	Sex	Age (y)	Tumor type	WHO grade	Biopsy or resection
1	M	34	Oligodendroglioma	II	Resection
2	F	61	Glioblastoma	IV	Resection
3	F	78	Glioblastoma	IV	Resection
4	M	67	Anaplastic astrocytoma	III	Biopsy
5	F	79	Glioblastoma	IV	Biopsy
6	M	57	Glioblastoma	IV	Biopsy
7	M	22	Astrocytoma	II	Resection
8	M	62	Glioblastoma	IV	Resection
9	F	47	Glioblastoma	IV	Resection
10	M	50	Oligoastrocytoma	II	Resection
11	M	37	Oligoastrocytoma	II	Resection
12	M	60	Anaplastic oligodendroglioma	III	Resection
13	F	65	Glioblastoma	IV	Resection
14	M	42	Oligodendroglioma	II	Resection
15	F	77	Glioblastoma	IV	Resection
16	F	34	Oligoastrocytoma	II	Resection
17	F	69	Glioblastoma	IV	Biopsy
18	M	77	Astrocytoma	II	Biopsy
19	M	59	Glioblastoma	IV	Resection
20	F	29	Oligodendroglioma	II	Resection
21	M	62	Anaplastic oligodendroglioma	III	Resection
22	F	74	Oligoastrocytoma	II	Biopsy
23	M	60	Anaplastic oligoastrocytoma	III	Resection
24	F	35	Glioblastoma	IV	Resection
25	M	51	Glioblastoma	IV	Resection
26	M	53	Glioblastoma	IV	Biopsy

Table 2. Imaging parameters of MRI acquisition protocol (Achieva 3T, Philips Healthcare)

Acquisition order	Sequence ^a	TR (ms)	TE (ms)	TI (ms)	Flip angle	no. of dynamics	Acquisition matrix	Thickness (mm)	Acquisition time
1	axial T2-w TSE	3000	80	-	90°	-	400×512	5	1 min 54 s
2	axial 3D-FLAIR	10000	110	2750	90°	-	224×256	2.5	8 min 20 s
3	axial 3D-T1w FFE	7.2	3.5	-	90°	-	256×256	2.5	1 min 22 s
4	axial Variable Flip Angle VFA	3.9	1.9	-	5°/10°/15°	-	96×112	2.5	2 min 3 s
5	axial dynamic gradient-echo T1-w DCE	3.9	1.8	-	15°	70	96×84	2.5	6 min 10 s
6	axial gradient-echo T2*-w EPI DSC	1500	40	-	75°	80	96×77	5	2 min 4 s
7	post-contrast axial 3D-T1w FFE	7.2	3.5	-	90°	-	256×256	2.5	1 min 22 s

Note: ^a TSE, turbo spin echo; 3D-FLAIR, three-dimensional fluid-attenuated inversion-recovery; 3D-FFE, three-dimensional fast-field echo; VFA, Variable Flip Angle; EPI, echo-planar imaging.

Table 3. Region of maximal abnormality (*hotspot*) values of rCBV, Vp and K^{trans} for different tumor grades.

	Grade II/LGG (n=9)	Grade III (n=4)	Grade IV (n=13)	HGG (n=17)	<i>p-value</i> ^a			
					II vs III	II vs IV	III vs IV	LGG vs HGG
$rCBV_{\text{max}}$	1.20 (0.80-5.00)	6.40 (2.20-7.00)	6.30 (4.20-9.00)	6.30 (2.20-9.00)	0.017*	<0.0001****	>0.05	<0.0001****
Vp_{max}	0.50 (0.30-1.90)	4.60 (2.60-6.40)	8.20 (5.70-14.70)	7.80 (2.60-14.70)	0.008**	<0.0001****	0.018*	<0.0001****
$K^{\text{trans}}_{\text{max}}$	0.004 (0.003-0.016)	0.105 (0.022-0.160)	0.130 (0.100-0.170)	0.120 (0.022-0.170)	0.008**	<0.0001****	>0.05	<0.0001****

Note: Data are interpatient median values, with range in parentheses.

^a Significant difference between groups ($P < 0.05$). *p*-values were calculated using Mann-Whitney U tests with Bonferroni correction for multiple comparisons. * $P \leq 0.05$, ** $P \leq 0.01$, *** $P \leq 0.001$, **** $P \leq 0.0001$

Table 4. Spearman's correlation between region of maximal abnormality (*hotspot*) values and tumor grade.

	ρ	<i>p-value</i>
$rCBV_{max}$	0.761****	<0.0001
Vp_{max}	0.893****	<0.0001
K_{max}^{trans}	0.818****	<0.0001

Note: Data are Spearman rank correlation coefficients (ρ). * $P \leq 0.05$, ** $P \leq 0.01$, *** $P \leq 0.001$, **** $P \leq 0.0001$

Table 5. Histogram measures for rCBV, Vp and ktrans in LGGs and HGGs.

		LGG	HGG	<i>p-value</i> ^a	AUC (CI 95%)^b	<i>p-value</i>
DSC rCBV	mean	1.351 ± 0.528	2.740 ± 0.930	0.001	0.928 (0.756-0.992)	<0.0001
	median	1.103 ± 0.371	2.274 ± 0.918	0.002	0.908 (0.729-0.985)	<0.0001
	SD	1.018 ± 0.606	1.976 ± 0.760	0.023	0.850 (0.656-0.958)	<0.001
	skewness	1.967 ± 0.715	1.410 ± 0.582	>0.05	0.752 (0.544-0.899)	0.025
	kurtosis	8.437 ± 7.154	3.455 ± 2.908	>0.05	0.771 (0.566-0.912)	0.008
	90th percentile	2.625 ± 1.289	5.374 ± 1.893	0.004	0.895 (0.712-0.980)	<0.0001
	95th percentile	3.322 ± 1.713	6.614 ± 2.384	0.015	0.863 (0.671-0.965)	<0.0001
DCE Vp	mean	1.057 ± 0.431	2.552 ± 1.328	<0.001	0.954 (0.793-0.998)	<0.0001
	median	0.756 ± 0.369	2.079 ± 1.226	<0.001	0.941 (0.774-0.996)	<0.0001
	SD	1.083 ± 0.719	1.922 ± 0.988	>0.05	0.824 (0.625-0.944)	0.001
	skewness	3.242 ± 1.475	1.701 ± 1.462	0.028	0.843 (0.648-0.955)	0.001
	kurtosis	21.54 ± 19.50	7.024 ± 17.03	0.018	0.856 (0.663-0.962)	<0.0001
	90th percentile	2.091 ± 0.868	5.016 ± 2.673	<0.001	0.948 (0.783-0.997)	<0.0001
	95th percentile	3.031 ± 1.553	6.212 ± 3.102	<0.001	0.876 (0.687-0.971)	<0.0001
DCE ktrans	mean	0.004 ± 0.003	0.027 ± 0.013	<0.0001	0.980 (0.833-1.000)	<0.0001
	median	0.002 ± 0.002	0.019 ± 0.013	0.001	0.928 (0.756-0.992)	<0.0001
	SD	0.006 ± 0.003	0.027 ± 0.011	<0.001	0.961 (0.802-0.999)	<0.0001
	skewness	6.100 ± 4.450	1.631 ± 1.054	0.004	0.895 (0.712-0.980)	<0.0001
	kurtosis	51.68 ± 57.57	4.412 ± 6.245	0.002	0.908 (0.729-0.985)	<0.0001
	90th percentile	0.009 ± 0.007	0.065 ± 0.031	0.0001	0.967 (0.812-1.000)	<0.0001
	95th percentile	0.013 ± 0.009	0.080 ± 0.034	0.0001	0.967 (0.812-1.000)	<0.0001

Note: Data are interpatient means ± standard deviations.

^a Significant difference between groups ($P < 0.05$). p -values were calculated using Mann-Whitney U tests with Bonferroni correction for multiple comparisons.

^b Data in parentheses are 95% binomial exact confidence intervals. Bold font indicate the best discriminating parameters.

Table 6. Spearman's correlation between histogram parameters from DSC and DCE and tumor grade.

	DSC rCBV		DCE Vp		DCE ktrans	
	ρ	<i>p-value</i>	ρ	<i>p-value</i>	ρ	<i>p-value</i>
mean	0.705****	<0.0001	0.795****	<0.0001	0.699***	0.001
median	0.633**	0.004	0.759****	<0.0001	0.584*	0.014
SD	0.596*	0.011	0.544*	0.032	0.698***	0.001
skewness	-0.420	>0.05	-0.642**	0.003	-0.591*	0.012
kurtosis	-0.435	>0.05	-0.677***	0.001	-0.620**	0.006
90th percentile	0.668**	0.002	0.783****	<0.0001	0.702**	0.001
95th percentile	0.605****	0.008	0.641***	0.003	0.696**	0.001

Note: Data are Spearman rank correlation coefficients (ρ), with Bonferroni correction. (* $P \leq 0.05$, ** $P \leq 0.01$, *** $P \leq 0.001$, **** $P \leq 0.0001$)

Table 7. ROC results of combined histogram values and their AUC for glioma grading.

	AUC^a	<i>p</i>-value
mean rCBV + 90th percentile rCBV	0.915 (0.738-0.988)	0.0004***
mean Vp + 90th percentile Vp	0.954 (0.793-0.998)	<0.0001****
mean ktrans + 90th percentile ktrans	0.967 (0.812-1.000)	<0.0001****
mean Vp + 90th percentile Vp + mean ktrans + 90th percentile ktrans	0.987 (0.844-1.000)	<0.0001****
mean Vp + 90th percentile Vp + mean ktrans + 90th percentile ktrans + mean rCBV + 90th percentile rCBV	1.000 (0.868-1.000)	<0.0001****

^a Data in parentheses are 95% binomial exact confidence intervals.

Figure 1
[Click here to download high resolution image](#)

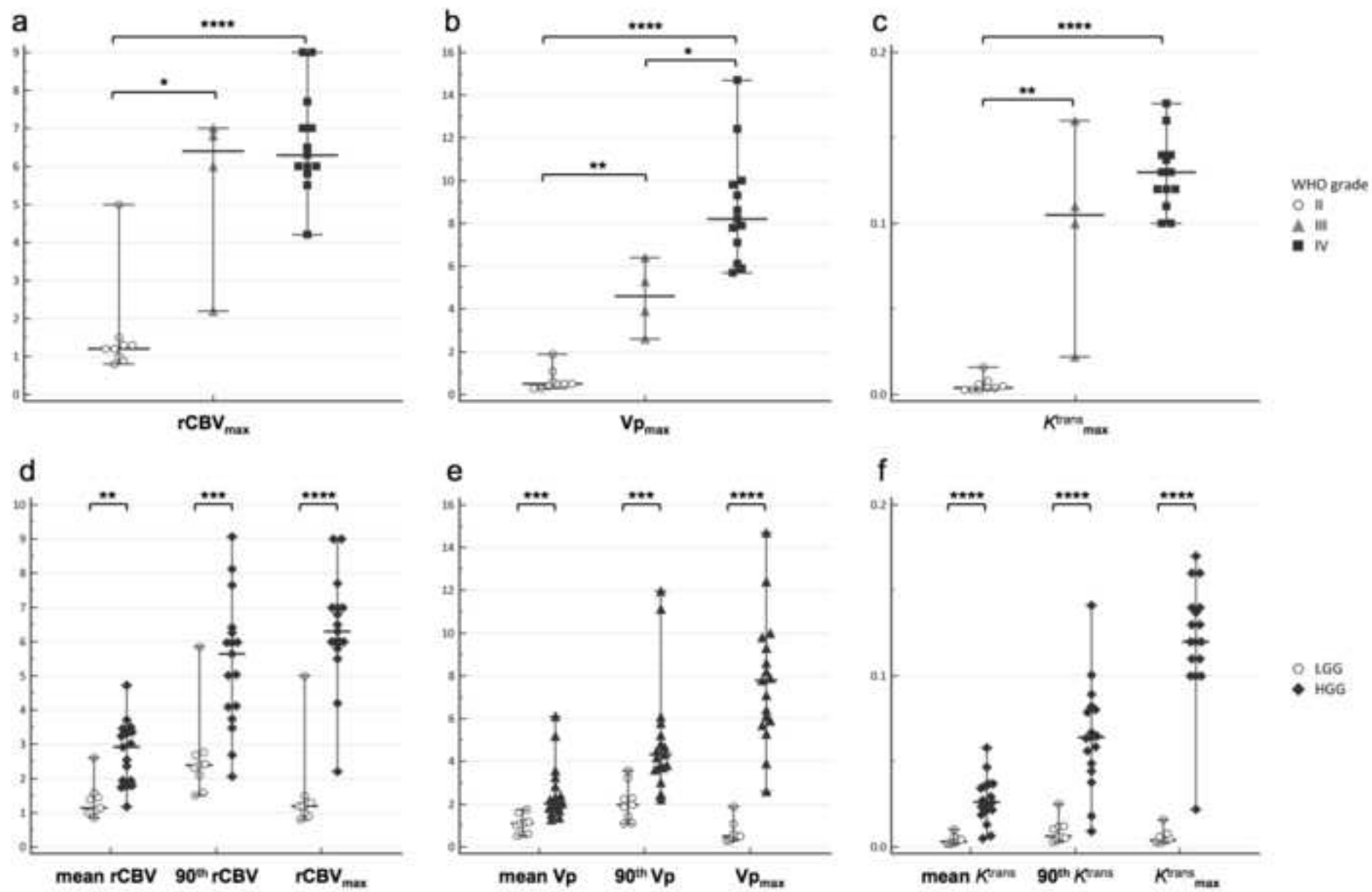


Figure 2
[Click here to download high resolution image](#)

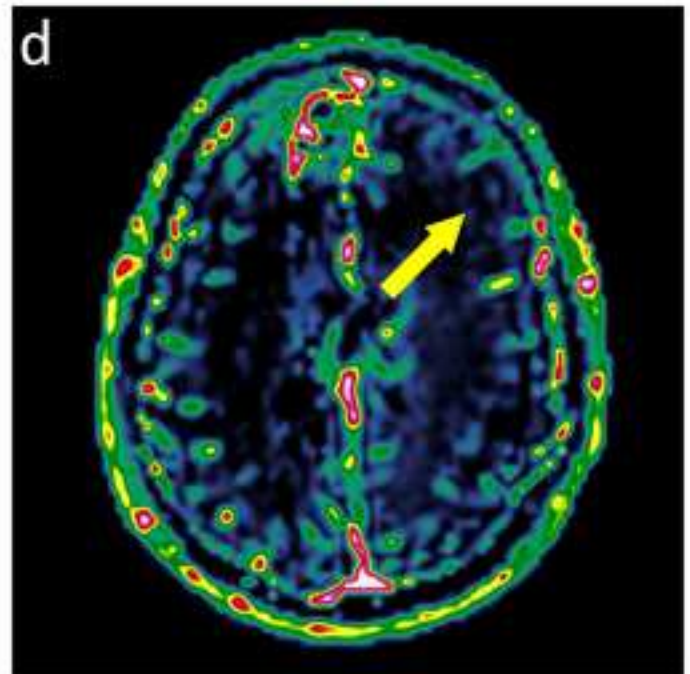
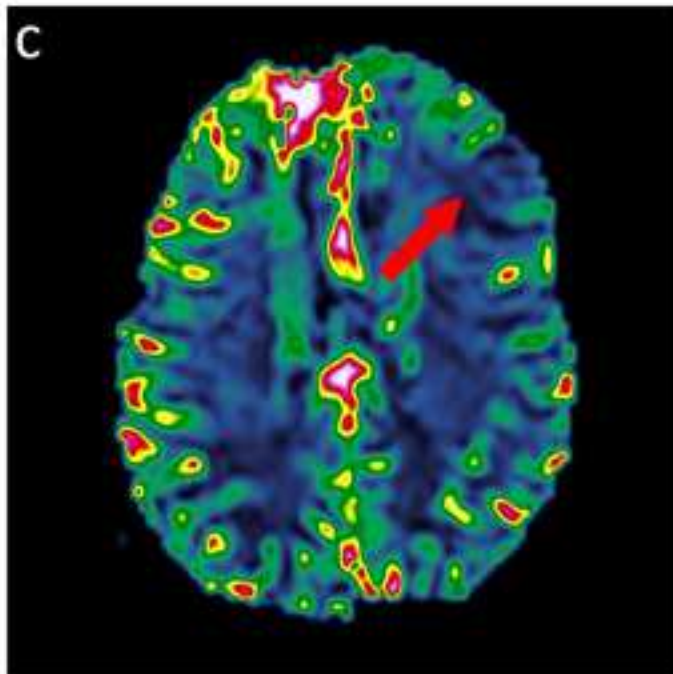
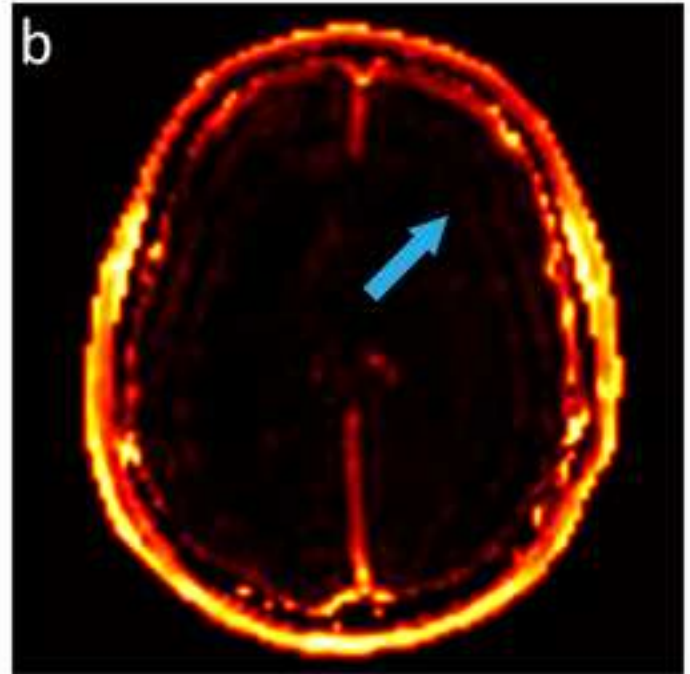
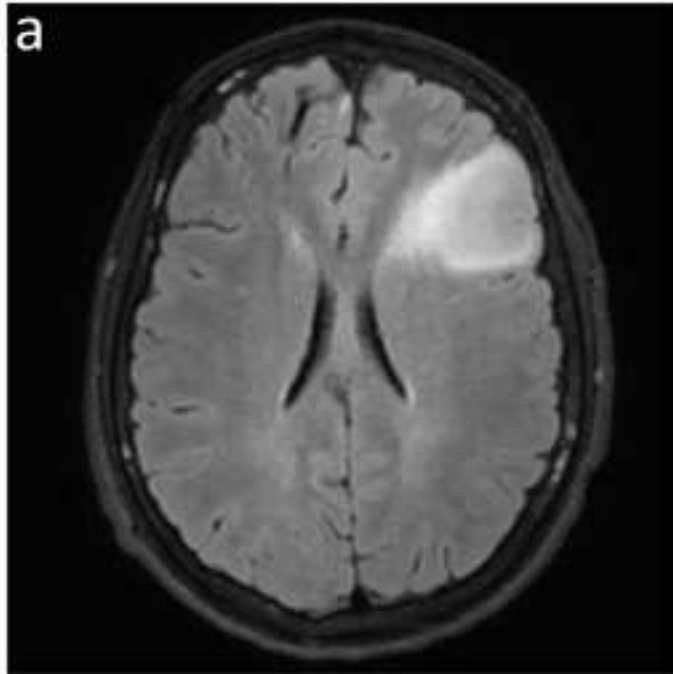


Figure 3
[Click here to download high resolution image](#)

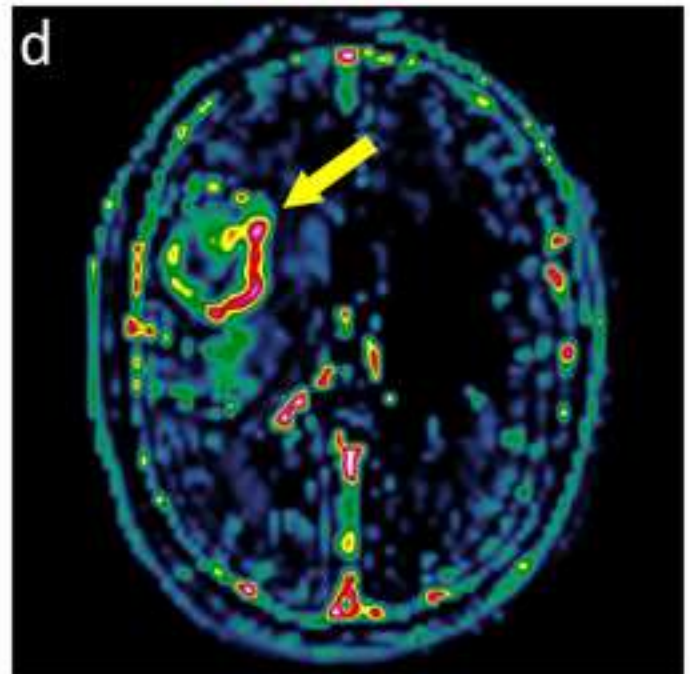
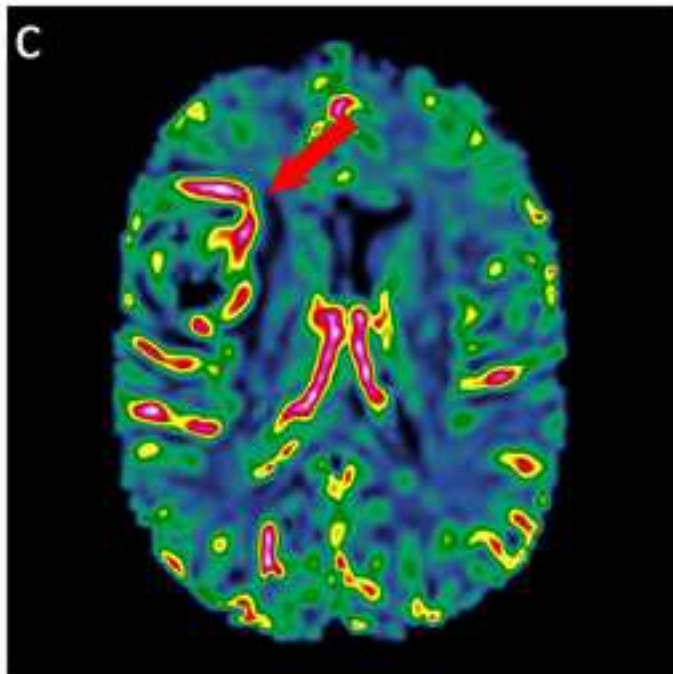
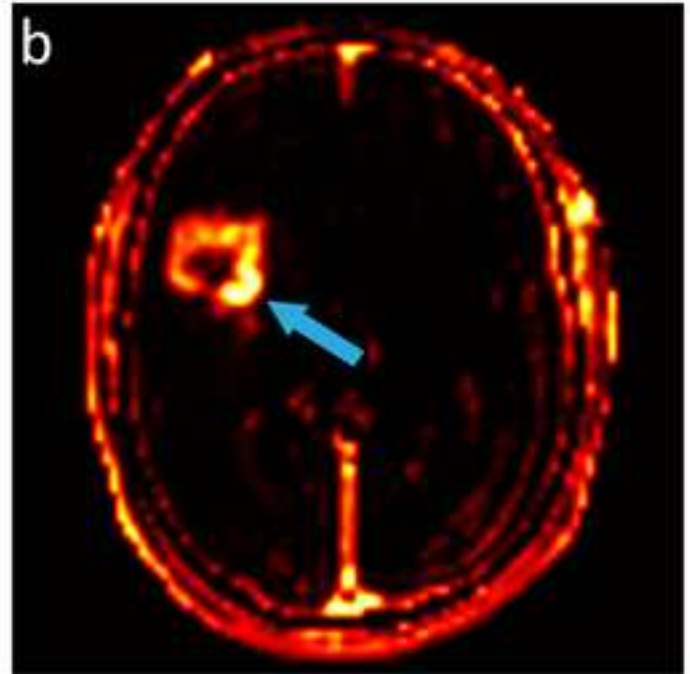
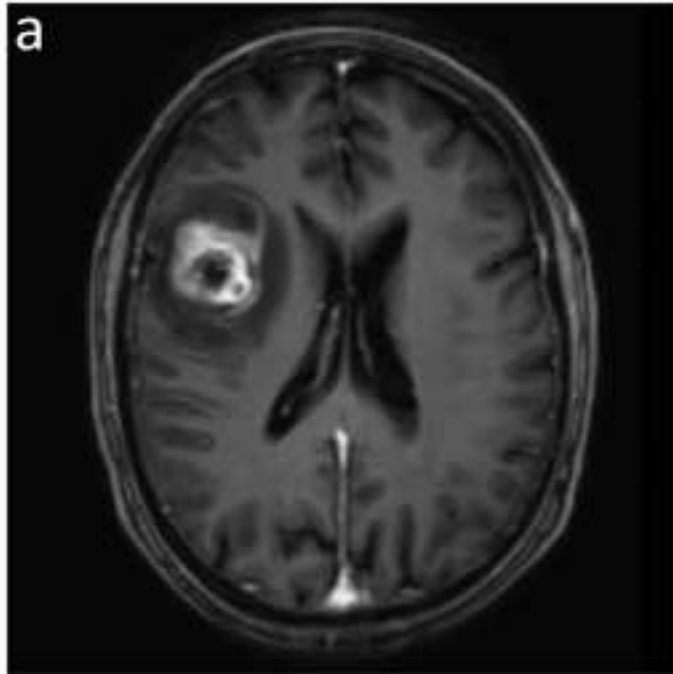


Figure 4
[Click here to download high resolution image](#)

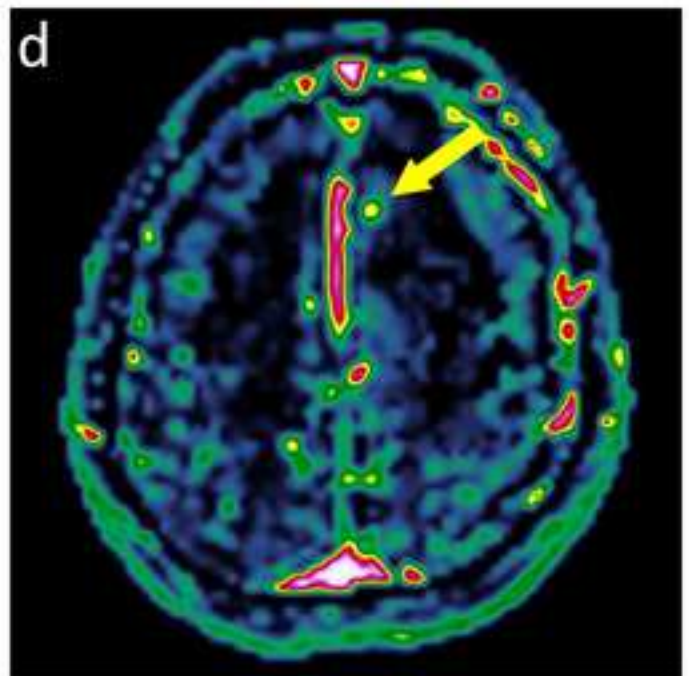
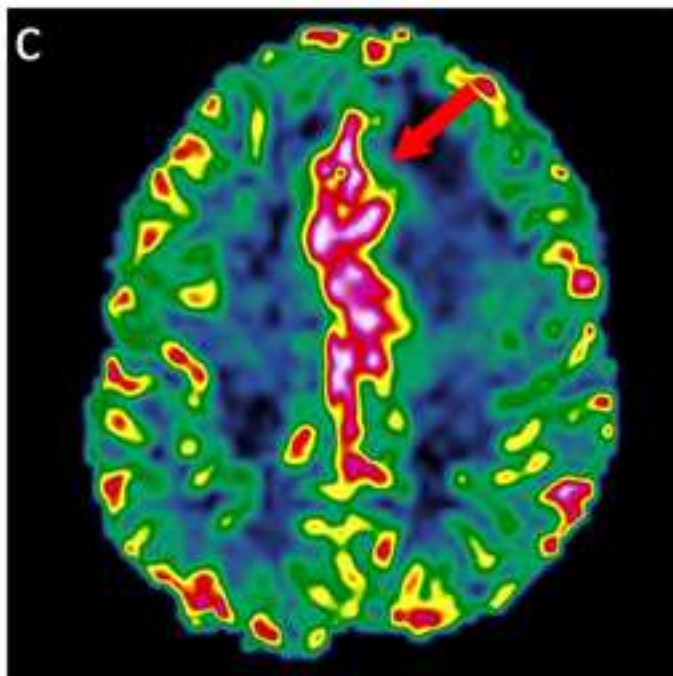
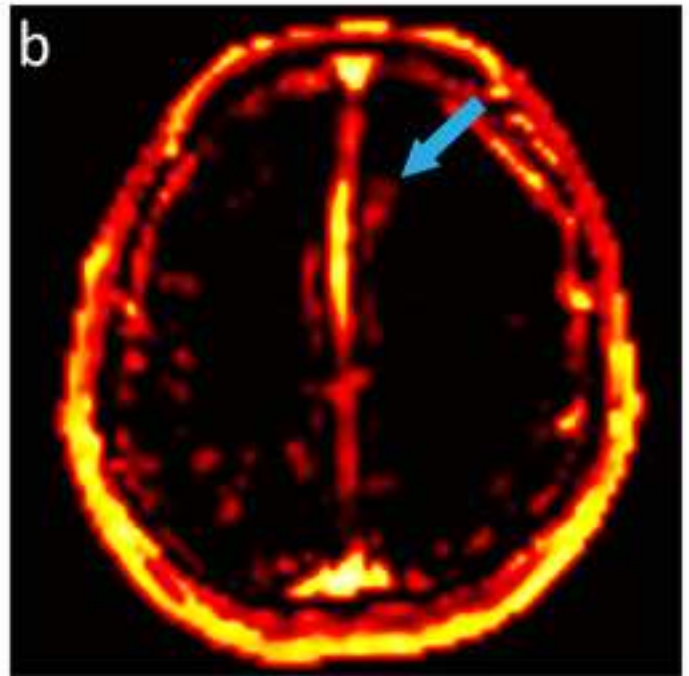
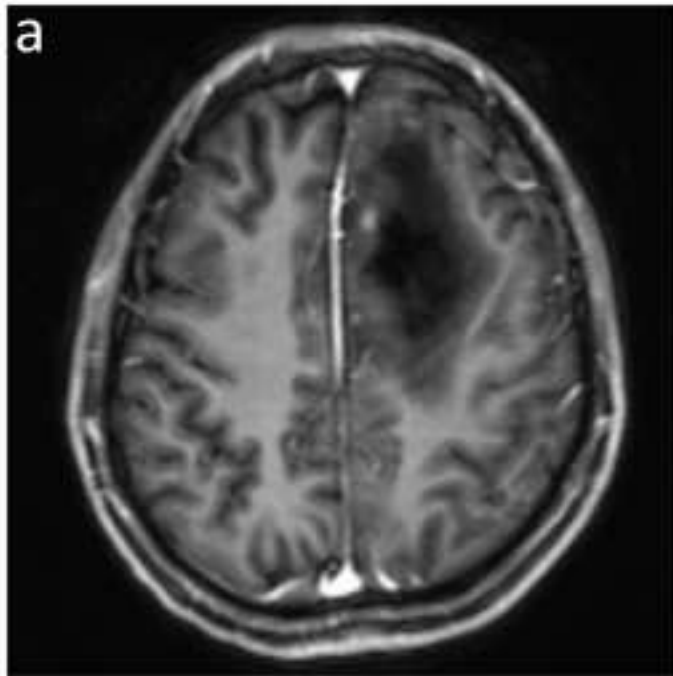
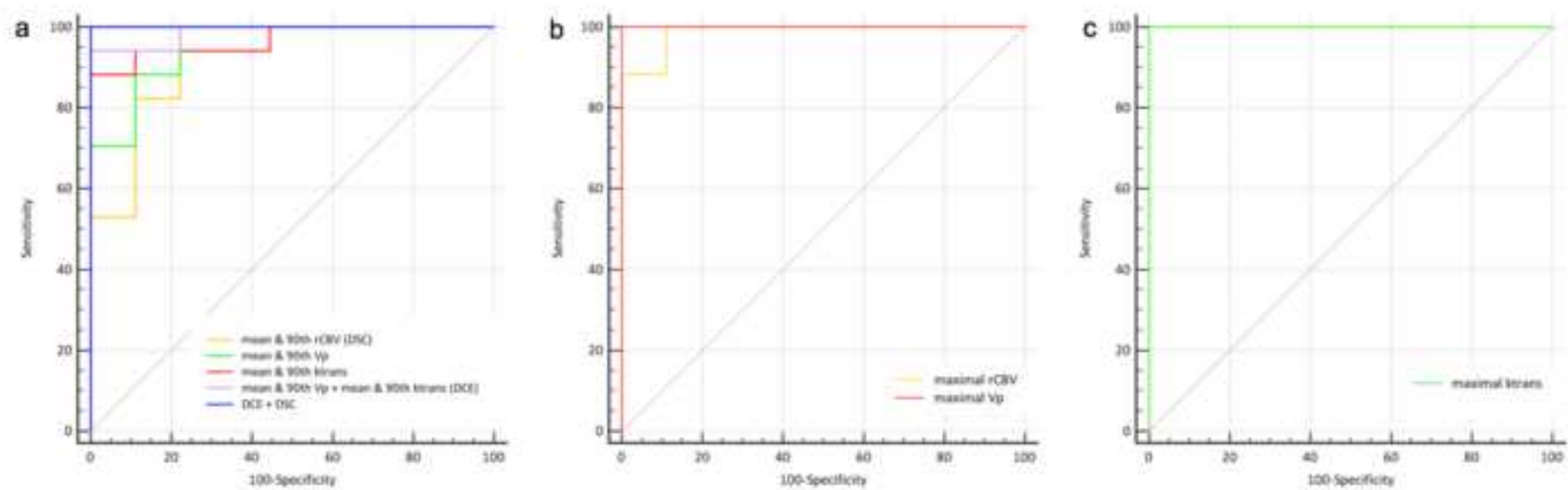


Figure 5
[Click here to download high resolution image](#)



Supplementary Table 1

[Click here to download Supplementary File\(s\): Supplementary_Table1.docx](#)